

Molecular Mechanochemistry: Low Force Switch Slows Enzymatic Cleavage of Human Type I Collagen Monomer

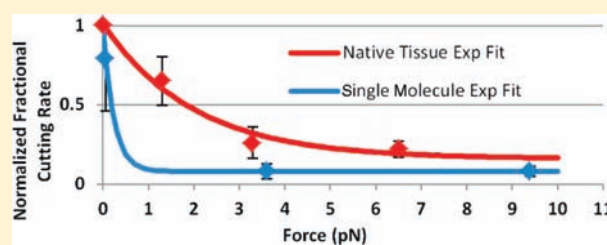
Robert J. Camp,[†] Melody Liles,^{†,§} John Beale,[‡] Nima Saeidi,[†] Brendan P. Flynn,[†] Elias Moore,[‡] Shashi K. Murthy,[‡] and Jeffrey W. Ruberti^{*,†}

[†]Department of Mechanical and Industrial Engineering and [‡]Department of Chemical Engineering, Northeastern University, 360 Huntington Avenue, Boston, Massachusetts 02115, United States

[§]School of Optometry and Vision Sciences, Cardiff University, Maindy Road, Cathays, Cardiff, F24 4LU, Wales, U.K.

S Supporting Information

ABSTRACT: In vertebrate animals, fibrillar collagen accumulates, organizes, and persists in structures which resist mechanical force. This antidissipative behavior is possibly due to a mechanochemical force-switch which converts collagen from enzyme-susceptible to enzyme-resistant. Degradation experiments on native tissue and reconstituted fibrils suggest that collagen/enzyme kinetics favor the retention of loaded collagen. We used a massively parallel, single molecule, mechanochemical reaction assay to demonstrate that the effect is derivative of molecular mechanics. Tensile loads higher than 3 pN dramatically reduced (10×) the enzymatic degradation rate of recombinant human type I collagen monomers by *Clostridium histolyticum* compared to unloaded controls. Because bacterial collagenase accesses collagen at multiple sites and is an aggressive cleaver of the collagen triple helical domain, the results suggest that collagen molecular architecture is generally more stable when mechanically strained in tension. Thus the tensile mechanical state of collagen monomers is likely to be correlated to their longevity in tissues. Further, strain-actuated molecular stability of collagen may constitute the fundamental basis of a smart structural mechanism which enhances the ability of animals to place, retain, and load-optimize material in the path of mechanical forces.



INTRODUCTION

Collagens are the dominant structural and most abundant protein in vertebrate animals, comprising 25–33% of their total protein mass.^{1,2} During development, growth, and remodeling of load-bearing connective tissue in vertebrate animals, fibrillar collagens are secreted and degraded continually.³ The continual turnover of collagen in load-bearing tissue is biased such that it results in the emergence of highly organized structures which are both stable and load-adapted. There is long-standing and substantial evidence that the macro- and microstructural adaptation of collagenous tissue rudiments to their loading environment is driven by epigenetic mechanobiological signaling.^{4–8} However, the precise mechanism which enables loaded collagen-based tissue to persist while adjacent unloaded tissue is preferentially removed is not known. Tensile mechanical strain is a robust signal which can directly alter the conformation and activity of cell adhesion molecules⁹ and collagen-associated extracellular matrix (ECM) molecular structures¹⁰ at low force levels. Although tension has been shown to directly or indirectly affect collagen and enzyme expression by extracellular matrix cells,^{11–16} very little is known about how strain alters enzymatic predilection for collagen. We have suggested previously that tensile strain, a persistent and low level guidance cue, is a regulatory signal for both collagen degradation and assembly.¹⁷ There is substantial data which demonstrates that strained, native collagenous tissue

exhibits enhanced resistance to enzymatic degradation in the absence of cells.^{18–21} Reconstituted collagen fibrillar networks under tensile strain have been shown to survive longer than unstrained fibrils in the presence of either bacterial collagenase^{17,22} or human neutrophil matrix metalloproteinase-8 (MMP-8).²³ However, it is not clear whether the strain-protection mechanism operates directly at the molecular level or if it is a consequence of strain-induced alterations in the molecular packing of collagen fibrils.²⁴ In this investigation, we sought to test the hypothesis that strain directly alters collagen/enzyme molecular interaction. The existence of molecular-level, force-actuated collagen stability raises the possibility that the collagen triple helix possesses an internal mechanism which naturally enhances its ability to form organized, load-bearing materials.

MATERIALS AND METHODS

A single molecule, mechanochemical enzyme cleavage assay, based on the simple, massively parallel magnetic tweezer system of Assi et al.²⁵ was adapted for this investigation. A stack of neodymium magnets is employed to provide an extremely stable, strong, laterally uniform magnetic field gradient on a population of superparamagnetic (SPM) beads.²⁵ The SPM beads are tethered to a glass surface with a molecular ‘chain’ of mechanochemical interest. In our case, type I recombinant human collagen

Received: November 21, 2010

Published: February 24, 2011

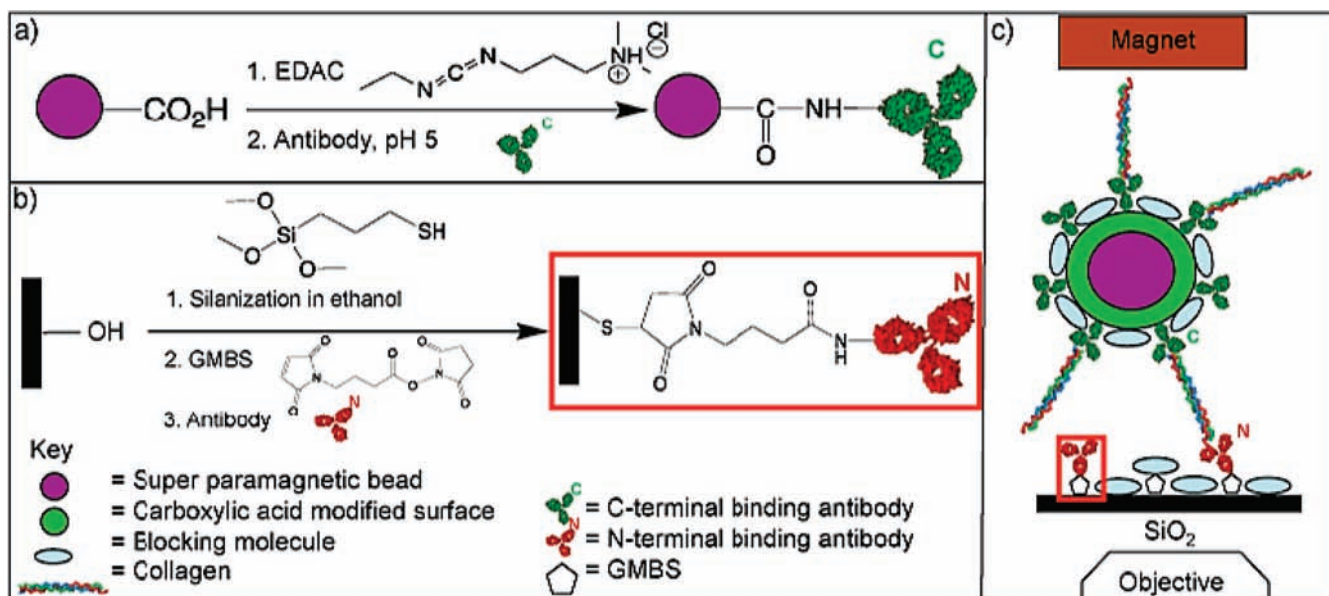


Figure 1. Experiment Chemistry. (A) Functionalization of the SPM beads with the C-terminal antibody. (B) Functionalization of the glass slides with the N-terminal antibody. (C) SPM bead tethered to the functionalized glass.

(rHCol1, RhC1-003, Fibrogen, San Francisco, CA) was bound via antibody²⁶ links to the beads and to the glass substrate (C and N terminal telopeptide antibodies were generously provided by Dr. Larry Fisher of the NIH.) Because the rHCol1, which is pepsin-extracted from a host culture, has partially degraded telopeptides (communication with Fibrogen, Inc.), capture of molecules with recognizable epitopes could only be reliably achieved by exposing antibody functionalized beads to enormous volumes of rHCol1. Antibody binding to rHCol1 was verified by SDS/Page, Western Blotting, and immunofluorescence microscopy (see Supporting Information (SI) for preparation details).

Figure 1a and b show the chemical sequence that was used to functionalize the beads and the glass with their respective antibodies (see SI for preparation details). Figure 1c is a schematic of the mechanochemical tethering system depicting the functionalized bead, collagen link, and functionalized glass as we expect it looks *in situ*. Multiple tethering of the beads was minimized by blocker/sparsing (see SI for preparation details) the antibodies on both the glass and the beads as described by Murthy et al.²⁷ We also performed a bead-tracking experiment to rule out spontaneous sticking and releasing by the tethered superparamagnetic bead as seen in some single DNA tether experiments²⁸ (see SI for preparation details). The tracking data clearly indicate a population of adhered but mobile beads on tethers. Enzyme activity on the link chemistry was shown to be minimal by exposing C and N terminal antibody-rabbit IgG tethered beads to collagenase and monitoring ejection rates (see SI for preparation details).

The experimental setup permits modulation of force on the collagen tethers by changing the height of the magnet above the glass surface to which the SPM beads are connected by the collagen link. Given the five neodymium magnet stack and 1 μm SPM beads, a maximum force of about 12 pN could be applied to the tethered beads with an estimated variation of 11% around the mean estimated force value (based on calibration results [see SI for preparation details]). Figure 2 is a schematic of the experimental apparatus used to conduct these massively parallel mechanochemical force assays. During the experiments, loaded (or unloaded) collagen-tethered beads are exposed to 5.56 μM enzyme (crude *Clostridium histolyticum*).

Time sequence images are taken of the constellation of beads which remain on the glass. The beads which remain are either collagenase ejectable (representing beads held to the surface by uncut collagen molecules) or nonspecifically bound. We have found, in general, that nearly all collagenase

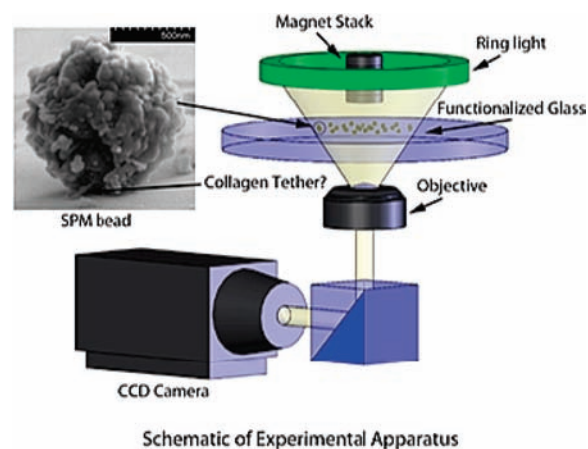


Figure 2. Schematic of the experimental setup. Superparamagnetic beads (1.0 μm diameter) are tethered to the functionalized glass by rhCol1 tethers. The force applied to the tethered beads is modulated (up to about 12 pN) by changing the height of the magnet stack. After a loaded control period, enzyme is added to the coverslip and the collagen-linked bead population decay is recorded by the CCD camera.

ejectable beads have been removed by the collagenase within 600 s (if one accounts for the spontaneous ejection rate) and stopped the data collection at that time point. The fraction of collagenase ejectable beads which remain on the glass at any time is plotted to generate population decay curves which typically exhibit decreasing exponential behavior, e^{-kt} . Under conditions of enzyme concentration in significant excess of k_m (the Michaelis–Menten constant), the rate constant, k , in the exponential is approximately equal to the catalysis rate of the enzyme/substrate pair $\sim k_{cat}$.²⁹ Though our enzyme concentration is not in significant excess of estimated values of k_m (5.56 vs 3.5 mM ³⁰), we performed auxiliary experiments at 50 mM and found no significant effect on the kinetics of the bead ejection rate. We thus felt comfortable using e^{-kt} as a model equation to fit the data sets.

The choice of forces used to load the collagen molecules was targeted to the mechanical regime where collagen begins its transition from purely entropic to more energetic strain values³¹ and where one might

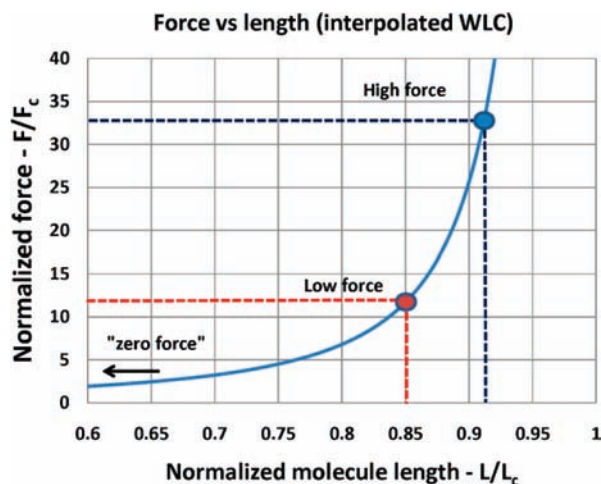


Figure 3. Normalized, interpolated WLC model for collagen force vs length curve showing location of our test loads (zero, low, and high force). The test forces span the region from low extension to fairly high extension of the monomer (i.e., from the entropic toward the elastic mechanical regime). F_c is the characteristic force for collagen defined as: $k_b T/L_p \approx 0.3$ pN. L_c is the contour length of the molecule ~ 309 nm.

expect a molecular stability transition. Equation 1 is the approximate interpolation equation for the entropic/elastic wormlike chain (WLC) model which relates the applied force on a single molecule to the displacement of the ends:³²

$$F_{WLC} = \frac{k_b T}{L_p} \left[\frac{1}{4 \left(1 - \frac{x}{L_c}\right)^2} - \frac{1}{4} + \frac{x}{L_c} \right] \quad (1)$$

where x is the end displacement and L_p and L_c are the persistence length and the contour length, respectively. Using the values for L_p (14.5 nm) and L_c (309 nm) that have been reported by Sun et al.,³¹ it is possible to estimate the end-to-end length of the collagen monomer while it is being stretched in our magnetic trap (Figure 3). Though we have used the collagen contour length, L_c , reported by Sun in our estimate, the collagen molecules in our trap are somewhat shorter as they do not have the terminal propeptides and are likely to be missing at least part of their telopeptides. Another uncertainty in the estimate is the contribution of the antibodies which were supplied to us as there is no available data on their length.

RESULTS

Using our massively parallel magnetic tweezer system, precise, small tensile forces were applied to collagen molecules in the presence of collagenase (see Materials and Methods section). The experimental series were divided into three categories (see Figure 3): “zero force” (Brownian tether forces ~ 0.06 pN, based on refs 28, 33); “low force” (averaging 3.6 ± 1.1 pN (s.d.)); and “high force” (averaging 9.4 ± 1.3 pN (s.d.)). The forces were achieved by changing the magnet stack heights to ∞ , 2.6 mm or 1.1 mm above the surface of the glass. Examination of the energetics of the force application in the range chosen suggest a sharp increase in the stiffness of the collagen monomer from the low to the high force while there is a smaller difference between the zero force and the low force (see Figure 3). Because of the rapid stiffness increase, we expected to see the major effect of force on the stability of the molecule to occur between the low and high force experiments.

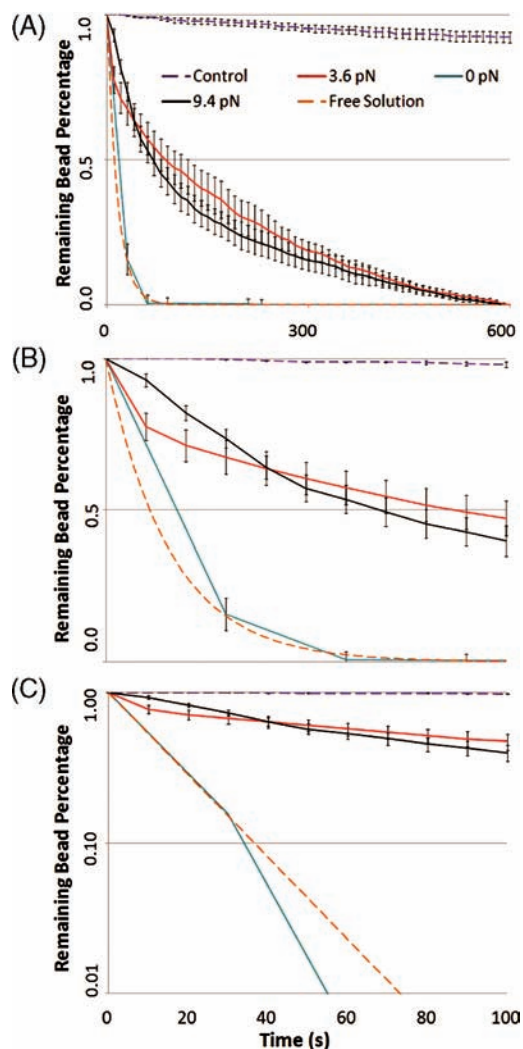


Figure 4. Force versus fractional rate of enzymatic cleavage of rhCol1 based on the fraction of collagenase-electable beads remaining on the glass as a function of time. Plots depict population decay curves reflecting the collagen/enzyme cleavage reaction rates for five cases: (1) Control (load and no enzyme); (2) 0 pN or “zero” force (enzyme and minimum load); (3) low force (3.6 pN and enzyme); (4) high force (9.4 pN and enzyme); and (5) theoretical curve reflecting collagen monomer degradation in free solution. Data for the theoretical curve are based on eq 25 in ref 29 and our enzymatic activity assay data for BC on rhCol1. (A) Entire experimental time course of 600 s. The theoretical and “zero” force curves show rapid loss of all collagen-linked beads within 100 s. For both the low and high force data, there is an initial rapid decline in collagen-linked bead population followed by a more consistent and slower rate of population decay. The rapid decay rate for the lower force is faster than that for the higher force, but the high and low force curves converge and track together with an exponential decay rate constant of 0.005/s. We suggest that this slower rate constant occurs where the beads are held to the glass by one molecule. The decay rate constant of the 0 pN force experiment is 0.05/s and is similar to the rate found by the free solution enzymatic assay of the rhCol1 (0.06/s). (B) Initial 100 s of the population decay data. (C) Semilog plot clearly shows different decay rate constants for each experiment (first 100 s).

The compiled experimental results are shown in Figure 4. The continuously extracted data from the high and low force runs generally show a classical exponential decay indicating the physics of the enzymatic cleavage process is governed by the law of equally

probable events. This is also consistent with the product formation equation (eq 25 in ref 29) and permits direct extraction of the enzymatic cutting rate by fitting the data with e^{-kt} .²⁹ Because the zero force data were obtained in a discrete manner (by periodically using the magnet stack to remove beads with cleaved collagen tethers) the separate data points were fitted with an exponential curve. In all, the three principal curves (high, low and zero force) comprise over 2500 individual observed cleavage events and represent an extremely robust data set.

Two control experiments were plotted: The first measured spontaneous ejections by exposing collagen tethered beads to a high force but not to enzyme (labeled “control”); the second experiment measured the basal catalysis rate of rhCol1 cleavage by BC in solution (labeled “free solution”) (see SI for methods details). The free solution control was run in our lab by separate investigators who were masked with regard to the zero force results. We used the extracted rate found in this second control to generate theoretical zero force ejection curves. In Figure 4, the data from the high load/no enzyme control show that there exists a small percentage of noncollagenase induced ejections and that the population of tethered beads decays at a rate of 0.0001/s ($r^2 = 0.99$) over the course of the experiment. These spontaneous ejections are to be expected and can be attributed to multiple factors including antibody bond relaxation and to detachment of some of the nonspecifically bound beads. The data from the control experiments run at zero load in free solution yielded a population decay curve which was produced using the experimentally determined activity ($k_{cat} \approx 0.063/s$) for collagen as the rate constant in the simple exponential decay equation e^{-kt} from ref 34. The curve depicts the expected population decay for mobile collagen in solution and reflects the cleavage rate for collagen in the totally entropic mechanical regime. It can be readily seen that the data obtained from the remaining experimental runs lay between the two control series.

The experimental series 3.6 and 9.4 pN force curves each exhibited an early slope change which was fitted with separate exponentials. Although we made every effort to minimize multiple collagen tethers, we cautiously attribute the slope change to a transition from a multiply tethered to a singly tethered population of beads. The multiple tether assumption is consistent with the observed increased initial rate of ejection because multiple tethers will effectively reduce the load per monomer. Note that the initial slope of the 3.6 pN data set nearly falls on the zero force control curve. An alternative explanation for the multiexponential behavior could be that the collagen/enzyme degradation reaction is a complex multistep hierarchical process which is partly force actuated. At this time it is impossible to isolate the reason for the multistep exponential response; however, regardless of the precise mechanism, the ejection rates are clearly force sensitive.

For the 9.4 pN force curve, the slope change occurs at approximately 40 s. Fitting the fast decay regime of the curve gives a k_{cat} of 0.011/s ($r^2 = 1.0$) while the fitting of the slow decay regime gives 0.005/s ($r^2 = 0.984$). The 3.6 pN force slope change occurs much more quickly (10 s into the experiment) and yields k_{cat} values of 0.028/s ($r^2 = 0.99$; fast decay regime) and 0.005/s ($r^2 = 0.998$; slow decay regime). It is important to note that both the high and low force experiments show similar ejection rates in their slow decay regimes (which we assume comprises ejections of beads with single tethers). This suggests that the effect of force does not alter the enzyme cutting rate significantly between 3.6 and 9.4 pN for single collagen tethers. The data obtained from the 0.0 pN experimental series, where the beads were collagen-tethered but unloaded, show a 10-fold increase in

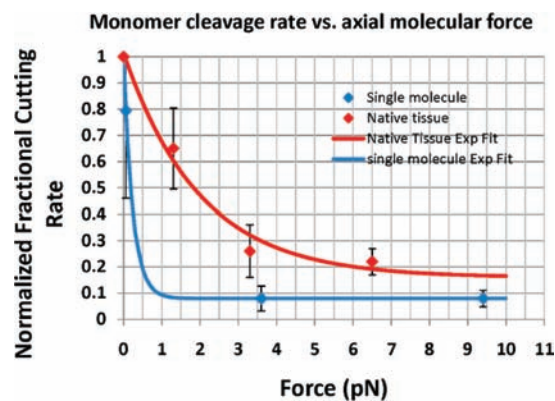


Figure 5. Monomer cleavage rate vs applied force comparison at the extremes of tissue hierarchy. The plot compares the effect of axial tensile load on the enzymatic cutting rate for the present single molecule investigation (blue diamonds) and for our native tissue investigation (red diamonds) published earlier this year (Zareian et al.²¹). The solid lines represent the fits of the discrete data with decaying exponential curves. The data show similar trends for the effect of force on the activity of the enzyme on single molecules and on molecules in native tissue. This is somewhat surprising given the complexity of native tissue architecture which in this case was a strip of bovine corneal stroma subjected to a uniaxial tensile load. The similarity in the trends suggests that the fundamental mechanochemical signature of the collagen/enzyme interaction is reflected in the whole tissue. Y-axis: normalized fractional rate of monomers cleaved; Normalization value was maximum cutting rate at zero force. Load on monomers in native tissue was estimated at the maximum enzymatic cleavage rate found in ref 21. The cleavage rate value for the native tissue at zero force was obtained by extrapolation from the data at the other three force values.

the rate of enzymatic digestion ($k_{cat} \approx 0.05/s$; $r^2 = 0.97$) relative to the low and high force series ($k_{cat} \approx 0.005/s$). The 0.0 pN enzymatic activity value is comparable to that found when unloaded rhCol1 is degraded in free solution ($k_{cat} \approx 0.06/s$). This correlation confirms that our molecular mechanochemical assay accurately captures standard collagen/enzyme kinetics when collagen is tethered to the SPM but unloaded. These curves are created from the pooled experimental data and fit to one master curve. This method gives us the most conservative rate of bead ejection. Individual experiment results were used to compare all force states for statistical significance, and it was found that the zero force and control curve were statistically different from each other and every force curve, while the 3.6 and 9.3 pN curves were not statistically different from each other.

DISCUSSION

The results are consistent with the hypothesis that mechanical strain is a potent regulator of collagen/enzyme interaction. We found that the presence of a small mechanical force (3.6 pN) applied to collagen molecular tethers profoundly enhances their resistance to enzymatic cleavage, but the resistance does not proportionally increase even when the force is raised by more than a factor of 2 to 9.4 pN. Though the experiment has been conducted using recombinant collagen in isolation, the results suggest that the strain-stabilizing effect which has been found in both native tissue^{18–21} and reconstituted collagen gels^{22,23} can be attributed, at least in part, to factors which occur at the molecular level. Figure 5 compares the present data to those extracted from the recent investigation of Zareian et al.²¹ which examined the effect of tensile mechanical force on the enzymatic degradation rate of native bovine corneal tissue strips. Both the single molecule and native tissue data

follow similar trends whereby increasing the load decreases the rate of enzyme conversion of the collagen. The data imply that the mechanochemical signature of the collagen/enzyme pair is reflected in the buildup of tissue hierarchy.³⁵ However, there are substantial differences between native tissue and our single molecule assay which could render the collagenolytic reaction in tissue less sensitive to force than exposed, loaded single collagen monomers. There is too little known about enzyme degradation in whole native tissue for us to speculate about why there is a difference in the sensitivity to force, so we choose to leave the question open for future investigations to resolve.

The most striking aspect of the data indicates that tensile mechanical loads cause a rapid switch in the state of the collagen monomer converting it from 'enzyme-susceptible' to 'enzyme-resistant' at relatively low force values. In addition, because bacterial collagenase aggressively attacks collagen at multiple sites³⁶ we conclude that tensile mechanical strain *generally* enhances collagen stability. A more general stability enhancement of the triple helix (rather than a specific effect such as changes in enzyme binding site conformation) is consistent with data obtained from investigations of collagen thermal denaturation. Such studies have shown collagen to be more resistant to thermal denaturation when under tensile strain and when packed into fibrils.^{37–39} The stability enhancement mechanism is not known but has been attributed to decreases in the configurational entropy of the monomers.⁴⁰

CONCLUSION

Objective examination of the development and growth of load-bearing structures in vertebrate animals suggests that collagen accumulates, organizes, and persists in regions which encounter mechanical force. We have recently postulated that this behavior is not completely cell-directed, but rather a consequence of collagen's mechanochemical signature which enhances its preferential retention when under load. Thus, the creation of structure in vertebrate animals could be viewed as a materials/mechanics problem as well as a biological one. The data presented in this investigation indicate that the force required to switch single collagen molecules from susceptible to resistant to enzymatic cleavage is relatively small. If this stability effect is also applicable to MMP/collagen interaction, even tissues under light loads may exhibit enhanced collagen stability and preferential fibril retention. One can readily imagine how load-adapted connective tissue structures might emerge during development given judicious application of mechanical strain to a growing structure in the presence of both catabolic molecules (enzymes) and anabolic molecules (collagen monomers). One may also imagine how tissues in which the mechanical environment changes over time (e.g., loss of protective tension on the collagen) might shed material through enzymatic action (e.g., osteoarthritis and intervertebral disk disease). Finally, mechanically controlled enzyme susceptibility may permit tissue engineers to optimize collagen-based constructs for regenerative medicine.

The low-force stability switch elucidated by this investigation may constitute the basis for a structural, smart material system which is antidissipative in that it automatically enables the generation of structures that are retained selectively in the path of mechanical force. The existence of such a mechanochemical mechanism could provide valuable insight into why collagens are present in virtually all animal phyla, why collagen is so well-conserved across evolution, and why collagen is the structural molecule of choice in vertebrate animals.

ASSOCIATED CONTENT

S Supporting Information. Experimental procedures. This material is available free of charge via the Internet at <http://pubs.acs.org>.

AUTHOR INFORMATION

Corresponding Author

j.ruberti@neu.edu

ACKNOWLEDGMENT

This study was partially supported by a grant from the National Institutes of Health: 1 R21 AR053551-01. R.J.C. was supported by the IGERT Nanomedicine Science and Technology program at Northeastern University (funding from NCI and NSF Grant 0504331). We would also like to thank Dr. Larry Fisher from the National Institute of Dental and Craniofacial Research for supplying the collagen antibodies used in this work.

REFERENCES

- (1) Hall, D. A. *International Review of Connective Tissue Research*; Academic Press: New York, 1964; Vol. 2.
- (2) Lehninger, A. L. *Biochemistry*, 2nd ed.; Worth Publishers, Inc.: New York, 1975.
- (3) Laurent, G. J. *Am. J. Physiol.* **1987**, *252*, C1–9.
- (4) Carter, D.; Beaupre, G. *Skeletal form and function: Mechanobiology of skeletal development, aging and regeneration*; Press Syndicate of the University of Cambridge: Cambridge, 2001.
- (5) Carter, D. R.; Van Der Meulen, M. C.; Beaupre, G. S. *Bone* **1996**, *18*, 5S–10S.
- (6) Chalmers, J.; Ray, R. J. *Bone Joint Surg.* **1962**, *44B*, 149–64.
- (7) Chamay, A.; Tschantz, P. J. *Biomech.* **1972**, *5*, 173–80.
- (8) Wolff, J. *Das Gesetz Der Transformation Der Knochen*; A Hirschwald: Berlin, 1891.
- (9) del Rio, A.; Perez-Jimenez, R.; Liu, R.; Roca-Cusachs, P.; Fernandez, J. M.; Sheetz, M. P. *Science* **2009**, *323*, 638–41.
- (10) Vogel, V.; Thomas, W. E.; Craig, D. W.; Krammer, A.; Baneyx, G. *Trends Biotechnol.* **2001**, *19*, 416–23.
- (11) Xu, Z.; Buckley, M. J.; Evans, C. H.; Agarwal, S. J. *Immunol.* **2000**, *165*, 453–60.
- (12) Parsons, M.; Kessler, E.; Laurent, G. J.; Brown, R. A.; Bishop, J. E. *Exp. Cell Res.* **1999**, *252*, 319–31.
- (13) Prajapati, R. T.; Chavally-Mis, B.; Herbage, D.; Eastwood, M.; Brown, R. A. *Wound Repair Regen.* **2000**, *8*, 226–37.
- (14) Prajapati, R. T.; Eastwood, M.; Brown, R. A. *Wound Repair Regen.* **2000**, *8*, 238–46.
- (15) Ragan, P. M.; Badger, A. M.; Cook, M.; Chin, V. I.; Gowen, M.; Grodzinsky, A. J.; Lark, M. W. *J. Orthop. Res.* **1999**, *17*, 836–42.
- (16) Wong, M.; Siegrist, M.; Goodwin, K. *Bone* **2003**, *33*, 685–93.
- (17) Bhole, A. P.; Flynn, B. P.; Liles, M.; Saeidi, N.; Dimarzio, C. A.; Ruberti, J. W. *Philos. Trans. R. Soc. London, Ser. A* **2009**, *367*, 3339–62.
- (18) Nabeshima, Y.; Groom, E. S.; Sakurai, A.; Herman, J. H. *J. Orthop. Res.* **1996**, *14*, 123–30.
- (19) Ruberti, J. W.; Hallab, N. J. *Biochem. Biophys. Res. Commun.* **2005**, *336*, 483–9.
- (20) Wyatt, K. E.; Bourne, J. W.; Torzilli, P. A. *J. Biomech. Eng.* **2009**, *131*, 051004.
- (21) Zareian, R.; Church, K. P.; Saeidi, N.; Flynn, B. P.; Beale, J. W.; Ruberti, J. W. *Langmuir* **2010**, *26*, 9917–26.
- (22) Huang, C.; Yannas, I. V. *J. Biomed. Mater. Res.* **1977**, *11*, 137–54.
- (23) Flynn, B. P.; Bhole, A. P.; Saeidi, N.; Liles, M.; DiMarzio, C. A.; Ruberti, J. W. *PLoS One* **2010**, *5*, e12337.
- (24) Orgel, J. P.; Irving, T. C.; Miller, A.; Wess, T. J. *Proc. Natl. Acad. Sci. U.S.A.* **2006**, *103*, 9001–5.

- (25) Assi, F.; Jenks, R.; Yang, J.; Love, C.; Prentiss, M. *J. Appl. Phys.* **2002**, *92*, 5584–5586.
- (26) Fisher, L. W.; Stubbs, J. T., 3rd; Young, M. F. *Acta Orthop. Scand. Suppl.* **1995**, *266*, 61–5.
- (27) Murthy, S. K.; Sin, A.; Tompkins, R. G.; Toner, M. *Langmuir* **2004**, *20*, 11649–55.
- (28) Nelson, P. C.; Zurla, C.; Brogioli, D.; Beausang, J. F.; Finzi, L.; Dunlap, D. *J. Phys. Chem. B* **2006**, *110*, 17260–7.
- (29) Tzafiriri, A. R.; Edelman, E. R. *J. Theor. Biol.* **2007**, *245*, 737–748.
- (30) Mallya, S. K.; Mookhtiar, K. A.; Van Wart, H. E. *J. Protein Chem.* **1992**, *11*, 99–107.
- (31) Sun, Y. L.; Luo, Z. P.; Fertala, A.; An, K. N. *Biochem. Biophys. Res. Commun.* **2002**, *295*, 382–6.
- (32) Marko, J. F.; Siggia, E. D. *Macromolecules* **1995**, *28*, 8759–8770.
- (33) Segall, D. E.; Nelson, P. C.; Phillips, R. *Phys. Rev. Lett.* **2006**, *96*, 088306.
- (34) Tzafiriri, A. R.; Bercovier, M.; Parnas, H. *Biophys. J.* **2002**, *83*, 776–93.
- (35) Perumal, S.; Antipova, O.; Orgel, J. P. *Proc. Natl. Acad. Sci. U.S.A.* **2008**, *105*, 2824–9.
- (36) Steinbrink, D. R.; Bond, M. D.; Van Wart, H. E. *J. Biol. Chem.* **1985**, *260*, 2771–6.
- (37) Bass, E. C.; Wistrom, E. V.; Diederich, C. J.; Nau, W. H.; Pellegrino, R.; Ruberti, J.; Lotz, J. C. *J. Biomech.* **2004**, *37*, 233–40.
- (38) Tiktopulo, E. I.; Kajava, A. V. *Biochemistry* **1998**, *37*, 8147–52.
- (39) Luescher, M.; Ruegg, M.; Schindler, P. *Biopolymers* **1974**, *13*, 2489–2503.
- (40) Miles, C. A.; Ghelashvili, M. *Biophys. J.* **1999**, *76*, 3243–52.